Journal of Thermal Analysis and Calorimetry
https://doi.org/10.1007/s10973-024-13323-0

Analysis of historical and future cooling degree days over Türkiye for facade design and energy efficiency in buildings

Ayşegül Bilgili[1] · Kasım Çelik[1] · Mehmet Bilgili[2]

Received: 9 August 2023 / Accepted: 19 May 2024
© The Author(s) 2024

Abstract
In today's examination of optimal facade design for buildings, facade performance has a significant influence on cooling energy consumption. Cooling degree days (CDD) is regarded as a basic and straightforward approach for predicting building cooling energy consumption. Accurate seasonal trend forecasting of the CDD plays a vital role in estimating the energy demand for building cooling. Unfortunately, there are no published statistics or research on Turkey's CDD data for the following years. The monthly mean CDD data of Türkiye were created in this study utilizing data from the Turkish State Meteorological Service for the historical period from 1991 to 2022. The Seasonal Autoregressive Integrated Moving Average (SARIMA) approach was used to model the CDD data, and a time series forecast was performed. The SARIMA model was used to forecast the future trend of CDD from 2023 to 2040. The monthly and yearly CDD statistics were presented as figures, while the yearly CDD maps for Türkiye were created using the ArcGIS software program. Finally, CDD zones that require more attention to the most appropriate facade design in terms of energy efficiency for buildings in Türkiye were identified and classified.

Keywords Building · Cooling degree day · Forecasting · Facade design · SARIMA model

Introduction

The most important clear goal of many energy–climate–environment policies in the world is to achieve net zero CO_2 emissions. The imperative to limit the global average air temperature increment to 2 °C or even 1.5 °C relative to the pre-industrial period would require global yearly CO_2 emissions to be net zero or net negative at the end of this century and maybe at the end of 2050. It is also known that the quantity of global warming rise is related to the total CO_2 emissions. For these reasons, achieving net zero emissions as a clear and absolute goal is becoming an increasingly important goal of energy, climate, and emissions politicians worldwide [1]. However, the energy needed in buildings today covers approximately 33% of the total global energy consumption (Fig. 1), and 27% of global greenhouse gas emissions originate from building energy operations [2].

Energy demand studies play a crucial role in designing a cost-effective and optimum design for a building's heating, ventilating, and air-conditioning (HVAC) units. Facades of buildings are becoming more significant than ever because of the goal of fulfilling energy demand with net zero emissions. The workload of the HVAC systems is decreased and aids in energy savings owing to the building facades created with the proper design. Determining the amount of degree days of heating and cooling (HDD and CDD) separately in the area where the building will be constructed is critical in terms of evaluating the HVAC system capacities and costs. In this sense, the CDD and HDD values are the most important impact indicators utilized to analyze the energy demand of buildings [3, 4]. Designers can integrate both active and passive cooling/heating techniques into the building faces they create while taking these indicators into account. It is essential to accurately analyze meteorological or climatic parameters in the design of indoor comfort qualities such as the cooling and heating conditions of buildings. In particular, for countries in the western hemisphere, the CDD and HDD

✉ Mehmet Bilgili
mbilgili@cu.edu.tr

[1] Department of Architecture, Faculty of Architecture, Cukurova University, 01330 Adana, Turkey

[2] Department of Mechanical Engineering, Ceyhan Engineering Faculty, Cukurova University, 01950 Adana, Turkey

Published online: 18 June 2024

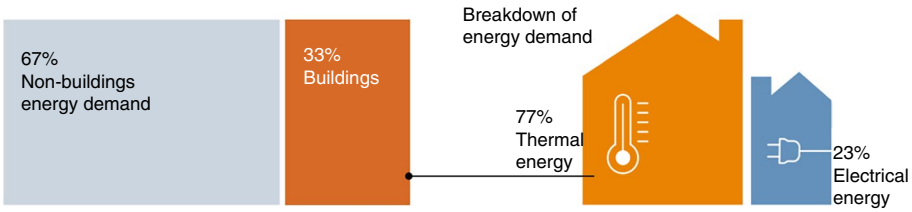


Fig. 1 Share of the global energy demand for buildings [2]

values play a critical role in the design of HVAC units, energy demand planning, and estimation of cooling and heating loads. Among several approaches for calculating monthly or annual energy demand, the degree-day technique is the simplest. Since the degree-day technique can provide a simple assessment of yearly energy demand, it is widely utilized in HVAC applications to predict the energy needs of cooling systems in the summer season and heating systems in the winter season [5].

Literature studies show that an increase in the heating or cooling needs of consumers will affect future energy demand. Due to climate change, extreme cold in the winter and overheating in the summer increase energy consumption, and depending on this increase, the heating and cooling costs of households or users also increase. Determining how much of this increase in energy costs is due to climate can only be done with the help of degree-day calculations. The number of hot days is used when calculating CDD, while the number of cold days is considered when calculating HDD. An increase in the number of high degree days indicates more intense heat or cold. A greater number of days also require more energy consumption to heat or cool a place. In this regard, it is crucial for future energy demand management to decrease energy demand costs and achieve maximum efficiency by accurately controlling environmental concerns related to energy consumption. Estimating and meeting the future energy consumption accurately are related to the most accurate forecasting of the cooling and heating demands due to climate change [6].

Globally, a decline in the number of heating days and a growth in the number of cooling days are predicted in the future. The net effects of these two usual extreme changes caused by the increase in average temperatures need to be scrutinized, especially in predicting the expected energy demand. Determining seasonal energy demand has critical importance in computing the cooling and heating demands of any building. Today, air-conditioning experts utilize design data in building energy demand analysis; therefore, they analyze cooling and heating situations in terms of interior thermal comfort design in buildings. HDD and CDD supply significant facilities for computing the building heating and cooling energy demands, designing the building facade to be used, energy management planning, and defining the size of HVAC units [7].

Related works

The time series analysis is classified into two types based on the total number of sample parameters at the time point: univariate and multivariate. Because of some complex features, modeling of time series and hence accurate time series estimation can become extremely difficult. In recent years, time series modeling and forecasting have become significant areas of study in engineering applications. Several distinct time series methods have been suggested in the literature, such as the autoregressive model [8, 9], the autoregressive integrated moving average (ARIMA) model [10–12], the support vector machine model [13, 14], and neural network-based techniques [15, 16]. Apart from these basic approaches, many hybrid methods [17, 18] have also been presented. Since time series datasets such as climate, financial, and seismic values are often non-stationary and nonlinear, these current techniques cannot virtually reveal sufficiently ordered data characteristics to yield accurate time series forecast results. Therefore, the deep learning approach, which has been accepted as a new technique that can accept a multilevel model of the original input by integrating simple but nonlinear modules, has been developed as a time series model. Because of these sufficient transformations, deep learning can learn all its properties from the input data at a sufficient level.

Degree-day methods have been widely presented in the literature by researchers in the energy analysis of buildings. As given in Table 1, HDD and CDD data were analyzed for different nations in international studies such as [19–36]. From the literature study, it was revealed that a study was conducted in two directions in terms of time in determining the HDD and CDD data. These are historical CDD and HDD trends and future CDD and HDD trends. Several scholars have investigated the historical tendencies of CDD and HDD data in different locations across the world using historical meteorological records. For example, Satman and Yalcinkaya [5] computed HDD and CDD data for 77 provinces throughout Türkiye. The HDD and CDD values were determined by Büyükalaca et al. [26] utilizing daily atmospheric temperature data from 78 cities throughout Türkiye. Using hourly atmospheric temperature data from 1983 to 1992, Papakostas and Kyriakis [23] calculated CDD and HDD data for two

Table 1 Some of the typical studies on the HDD and CDD estimations

References	Study area and trend	Country	Data time
Işık et al. [3]	HDD and CDD-Machine Learning	Türkiye	last 11 years
Satman and Yalcinkaya [5]	Historical HDD and CDD	Türkiye	Since 1991
Kuru and Calis [6]	HDD- Machine Learning	France	1974–2017
Dombaycı [7]	Historical HDD and CDD	Türkiye	1985–2005
De Rosa et al. [19]	Historical HDD and CDD	Italy	1978–2013
Sadeqi et al. [20]	Historical HDD and CDD	Iran	1960–2019
Yildiz and Sosaoglu [21]	Historical HDD and CDD	Türkiye	1975–2004
Al-Hadhrami [22]	Historical HDD and CDD	Saudi Arabia	1970–2006
Papakostas and Kyriakis [23]	Historical HDD and CDD	Greece	1983–1992
Idchabani et al. [24]	Historical HDD and CDD	Morocco	2000–2009
Jiang et al. [25]	Historical HDD and CDD	China	1959–2004
Büyükalaca et al. [26]	Historical HDD and CDD	Türkiye	1980–1998
Livada et al. [27]	Historical HDD and CDD	Australia	1999–2019
Li et al. [28]	Historical HDD	Global	1970–2018
Indraganti and Boussaa et al. [29]	Historical HDD and CDD	Saudi Arabia	2005–2014
Amber et al. [30]	Historical HDD and CDD	Pakistan	1985–2015
Ramon et al. [31]	Future HDD and CDD	Belgium	2070–2098
OrtizBeviá et al. [32]	Future HDD and CDD	Spain	2001–2050
Andrade et al. [33]	Future HDD and CDD	Portugal	2006–2070
Ukey and Rai [34]	Future HDD and CDD	India	2018–2100
Corrales-Suastegui et al. [35]	Future HDD	Mexico	2041–2060 2080–2099
Spinoni et al. [36]	Future HDD and CDD	Europe	1981–2100

cities in Greece. Yildiz and Sosaoglu [21] used data over 30 years from 1975 to 2004 to report yearly and monthly HDD and CDD data for 100 unique localities in Türkiye. Jiang et al. [25] used data on atmospheric temperature values recorded at 51 meteorological observations between 1959 and 2004 to calculate yearly and seasonal CDD and HDD data in Xinjiang, China. With the help of 21-year (from 1985 to 2005) daily maximum and lowest outdoor temperature data for 79 cities, Dombaycı [7] estimated the CDD and HDD data based on various base air temperatures and ultimately produced an HDD and CDD map of Türkiye. Al-Hadhrami [22] used daily average atmospheric temperatures at 38 meteorological points to report annual and seasonal CDD and HDD data in the Kingdom of Saudi Arabia. Maps of the CDD and HDD for Morocco were produced by Idchabani et al. [24] using information from 37 meteorological stations during a 10-year period from 2000 to 2009. De Rosa et al. [19] used daily averaged meteorological data from 1978 to 2013 to study the present situation and historical tendency of HDD and CDD in Italy. Using historical data from 2005 to 2014, Indraganti and Boussaa [29] presented CDD and HDD data for several cities in Saudi Arabia. Using 30-year long-term collected data, Amber et al. [30] calculated annual CDD and HDD levels in several Pakistani locations. For the years 1999 through 2019 in Australia, Livada et al. [27] examined the heating and cooling degree hours utilizing ambient air temperature and wind direction. The distribution of HDDs worldwide, and their interannual variations and significant factors during 1970–2018, was investigated by Li et al. [28]. Sadeqi et al. [20] examined the temporal trends and change points in HDD, CDD, and their simultaneous combination (HDD + CDD) in Iran, spanning a 60-year period between 1960 and 2019. Using the idea of dehumidification degree days based on moisture content, Cao et al. [37] examined the degree days over the previous 57 years for temperature decline and dehumidification in four cities belonging to key climate zones in China. To establish climate zones, Omarov et al. [38] suggested a novel method based on HDD, CDD, and building energy performance. The authors chose 90 provinces from 18 climate zones around the world for this purpose, and utilizing hourly weather data files from two separate record periods (2004–2018 and 2016–2020), they estimated and compared the DD values. Using data for the years 1979–2021, Pangsy–Kania et al. [39] examined the effects of climate

change, or global warming, on the number of HDD and CDD as well as the weather-related final energy consumption of European households (EU–27 and Norway). On the basis of daily temperature measurements from 27 sites in Bangladesh, Islam et al. [40] investigated the trend and variability of CDD and HDD and their potential causes for fluctuation throughout the study period 1980–2017. Al-Saadi et al. [41] used monthly average temperature data from 2005 to 2015 to calculate the CDD and HDD for 31 meteorological stations in Oman. Using the average monthly temperature data for the years 2017–2021, Salem et al. [42] provided the CDD values for the capitals of the Gulf Cooperation Council (GCC).

Several studies have predicted future CDD and HDD values utilizing future climate data in addition to analyzing historical CDD and HDD trends. For instance, Ortiz-Beviá et al. [32] studied CDD and HDD data for the years 2001–2050 after first calculating HDD and CDD data from 1958 to 2005 for Spain using air temperatures from 31 sites. Spinoni et al. [36] used regional climate models to investigate the spatial dispersal and quantification of possible significant differences in CDD and HDD data between 1981 and 2100. Ramon et al. [31] analyzed CDD and HDD data in Belgium utilizing hourly mean atmospheric temperatures from 1976 to 2004 for the recent past and 2070 to 2098 for the future. Ukey and Rai [34] analyzed the future and past developments of annual HDD and CDD data from 1969 to 2017 and 2018 to 2100 using weather data. Bilgili et al. [43] used SARIMA and LSTM models to predict HDD data for one month ahead and their short-term future. Bilgili [44] first created the SARIMA model to predict CDD data in different areas with a high cooling need in Türkiye and then predicted the future tendencies of the CDD data between 2022 and 2031. Karagiannidis et al. [45] used regional climate models/general circulation models (RCM/GCM) simulations under two representative concentration paths (RPC4.5 and RPC8.5) to study changes in HDD and CDD in Greece in the near future (2021–2050). Karagiannidis et al. [46] presented maps of average annual CDD and HDD deviations under RCP4.5 and RCP8.5 for the period 2023–2030 compared with the reference period 1991–2020. Mehmood et al. [47] aimed to calculate Pakistan's cooling degree days based on the heat index for the years 2050 and 2080 as well as the present.

Artificial intelligence techniques based on time series approaches have been widely employed in the estimation of weather or climate sciences in recent years. Autoregressive (AR) models, such as the ARIMA model and its derivatives, are used in traditional time series approaches. According to the literature survey, there is a little research on the use of artificial intelligence algorithms to determine CDD and HDD values. Kuru and Calis [6], for example, forecasted the monthly mean HDD data over France using a time series technique based on the SARIMA method. Işık et al. [3] estimated HDD and CDD data for 50 provinces of Türkiye utilizing artificial neural networks (ANN) and an adaptive network-based fuzzy inference system (ANFIS) and created a Türkiye map.

In the literature, the HDD and CDD data needed by the energy sector are generally calculated analytically according to a certain base atmospheric air temperature. Recent studies have dealt with the degree-day projection of future years for different global regions [31–34]. However, in these studies, future air temperature data under predicted future global warming are needed to predict HDD and CDD data. Furthermore, the determination of these meteorological data for future years is obtained using an estimation result. However, studies on the time series approach to identify HDD and CDD data for future years are limited. To the best of our knowledge, there are no published studies on the analysis of the future tendency of CDD for Türkiye to date. This work presents a model for forecasting monthly CDD data and future prediction of a data-driven CDD based on a classical (statistical) time series forecasting approach. In this study, a time series forecasting model with a very small margin of error is developed for monthly and yearly CDD time series for Türkiye. In this approach, there is no need for extra meteorological information. The developed SARIMA model is used to estimate future CDD data for Türkiye. With the SARIMA model, the future trend of CDD is forecasted for the period 2023–2040. The Engle autoregressive conditional heteroscedasticity (ARCH) test and Augmented Dickey–Fuller (ADF) test in determining, choosing, and assessing models for CDD data are used. Finally, future CDD estimations with an approximately 95% estimation interval are produced for the 216-month period from the proposed SARIMA model. The novelty and purpose of the study are summarized as follows:

- to analyze the historical trend and current state of CDD in Türkiye from 1991 to 2022,
- to forecast the future trend of CDD for Türkiye from 2023 to 2040,
- to present yearly CDD maps for Türkiye using the ArcGIS software program,
- to develop a model based on a classical time series forecasting approach for monthly CDD data in Türkiye,
- to classify CDD zones in Türkiye in terms of facade design and energy efficiency for cooling energy demand in buildings.

Methods

Cooling degree day

Degree day is defined as the amount of energy necessary to heat and cool buildings [48]. CDD for an n-day is expressed as [25]:

$$\mathrm{CDD} = \sum_{i=1}^{n} \left(T_{\mathrm{meani}} - T_{\mathrm{bc}}\right)^{+} \tag{1}$$

where T_{mean} and T_{bc} are the daily average atmospheric temperature value and the reference (base) temperature value, respectively. T_{bc} is considered to be 22 °C for this study. The units of CDD and temperature are the same [25, 49].

ARIMA model

ARIMA model, commonly comprehended as Box and Jenkins models, is one of the statistical approaches used for forecasting the future. Autoregressive Models (AR) are methods that represent the observation value of a time series at any period as a linear computation of the same series' observation value for a given number of periods before it and the error term. Moving Average Models (MA) are time series models in which the observation value in each period is stated as a linear combination of the same period's error terms and the error terms of a given number of previous periods. Autoregressive Moving Average Models (ARMA) are a blend of AR and MA models that are utilized to model stationary time series. The observation value of any period of a time series is described in these models as a linear combination of a predetermined number of prior observation values and the error term [10, 11]. An ARIMA model is defined as [50]:

$$\Delta^{\mathrm{D}} y_{\mathrm{t}} = c + \Delta^{\mathrm{D}} \phi_1 y_{\mathrm{t-1}} + \cdots + \phi_{\mathrm{p}} \Delta^{\mathrm{D}} y_{\mathrm{t-p}} + \varepsilon_{\mathrm{t}} + \theta_1 \varepsilon_{\mathrm{t-1}} + \cdots + \theta_{\mathrm{q}} \varepsilon_{\mathrm{t-q}} \tag{2}$$

where $\Delta^{\mathrm{D}} y_{\mathrm{t}}$ is a Dth differenced time series. p is the AR degree and denotes the number of past observations. q is the MA degree and expresses the number of past innovations. An ARIMA model can also be stated in lag operator notation as follows:

$$\phi^{*}(L) y_{\mathrm{t}} = \phi(L)(1-L)^{\mathrm{D}} y_{\mathrm{t}} = c + \theta(L)\varepsilon_{\mathrm{t}} \tag{3}$$

where ϕ^{*} is a polynomial with exactly D unit roots and an unstable AR operator. The nonseasonal differencing operator, $(1-L)^{\mathrm{D}}$, adjusts for nonstationarity in data collected throughout time.

SARIMA model

The SARIMA model is an ARIMA extension that deals with seasonality and probable seasonal unit roots. The SARIMA model is described as multiplicative ARIMA$(p,D,q)x(p_s,D_s,q_s)$ for a series with periodicity s and is alternatively defined as [50]:

$$\phi(L)\Phi(L)(1-L)^{\mathrm{D}}(1-L^{\mathrm{s}})^{\mathrm{D_s}} y_{\mathrm{t}} = c + \theta(L)\Theta(L)\varepsilon_{\mathrm{t}} \tag{4}$$

where D_{s} denotes the seasonal integration degree. $(1-L^{\mathrm{s}})^{\mathrm{D_s}}$ is the seasonal differencing operator and expresses the nonstationarity in data measured in the same period at successive times. $\Phi(L)$ is a stable and degree p_{s} AR operator of the $\phi(L)$ form. Also, $\Theta(L)$ is an invertible and degree q_{s} MA operator of the $\theta(L)$ form. The SARIMA method is described by Box and Jenkins [50] in detail.

Model evaluation metrics

To assess the prediction performance of the constructed model, the root-mean-square error (RMSE), mean absolute error (MAE), and correlation coefficient (R) were utilized. The required equations are expressed in Eqs. (5)–(7) [51]:

$$\mathrm{RMSE} = \sqrt{\frac{1}{n}\sum_{i=1}^{n}\left(\hat{y}_{\mathrm{i}} - y_{\mathrm{i}}\right)^2} \tag{5}$$

$$\mathrm{MAE} = \frac{1}{n}\sum_{i=1}^{n}\left|\hat{y}_{\mathrm{i}} - y_{\mathrm{i}}\right| \tag{6}$$

$$R = \left(1 - \frac{\sum_{i=1}^{n}\left(\hat{y}_{\mathrm{i}} - y_{\mathrm{i}}\right)^2}{\sum_{i=1}^{n}\left(\bar{y}_{\mathrm{i}} - y_{\mathrm{i}}\right)^2}\right)^{1/2} \tag{7}$$

where $\hat{y}_{\mathrm{i}}$, y_{i}, and $\bar{y}_{\mathrm{i}}$ present the estimated, actual, and mean values, respectively.

Table 2 Geographical data of the 81 measurement stations or cities considered in the study

Meteorological station	Latitude/°	Longitude/°	Altitude/m	CDD 2022/°C year^{-1}
Adana	37.0041	35.3443	23	863
Adıyaman	37.7553	38.2775	672	1036
Afyonkarahisar	38.7380	30.5604	1034	88
Ağrı	39.7253	43.0522	1646	156
Amasya	40.6668	35.8353	409	242
Aksaray	38.3705	33.9987	970	252
Ankara	39.9727	32.8637	891	229
Antalya	36.9063	30.7990	64	800
Ardahan	41.1061	42.7055	1827	1
Artvin	41.1752	41.8187	613	111
Aydın	37.8402	27.8379	56	788
Balıkesir	39.6500	27.8666	102	287
Bartın	41.6248	32.3569	33	142
Batman	37.8636	41.1562	610	889
Bayburt	40.2547	40.2207	1584	41
Bilecik	40.1414	29.9772	539	85
Bingöl	38.8847	40.5007	1139	428
Bitlis	38.4750	42.1625	1785	134
Bolu	40.7329	31.6022	743	4
Burdur	37.7220	30.2940	957	275
Bursa	40.2308	29.0133	100	315
Çanakkale	40.1410	26.3993	6	390
Çankırı	40.6082	33.6102	755	188
Çorum	40.5461	34.9362	776	92
Denizli	37.7620	29.0921	425	659
Diyarbakır	37.8973	40.2027	674	938
Düzce	40.8437	31.1488	146	157
Edirne	41.6767	26.5508	51	436
Elazığ	38.6443	39.2561	989	547
Erzincan	39.7523	39.4868	1216	290
Erzurum	39.9529	41.1897	1758	23
Eskişehir	39.7656	30.5502	801	73
Gaziantep	37.0585	37.3510	854	740
Giresun	40.9227	38.3878	38	209
Gümüşhane	40.4598	39.4653	1216	75
Hakkâri	37.5745	43.7388	1727	344
Hatay	36.2048	36.1513	104	563
Iğdır	39.9227	44.0523	856	511
Isparta	37.7848	30.5679	997	243
İstanbul	40.9113	29.1558	18	318
İzmir	38.3949	27.0819	29	728
Kahramanmaraş	37.5760	36.9150	572	767
Karabük	41.1961	32.6213	400	86
Karaman	37.1932	33.2202	1018	174
Kars	40.6042	43.1073	1777	9
Kastamonu	41.3710	33.7756	800	22
Kayseri	38.6870	35.5000	1094	142
Kırıkkale	39.8433	33.5181	751	352
Kırklareli	41.7382	27.2178	232	255
Kırşehir	39.1639	34.1561	1007	294
Kilis	36.7085	37.1123	640	799
Kocaeli	40.7663	29.9173	74	308
Konya	37.9837	32.5740	1031	184
Kütahya	39.4171	29.9891	969	33
Malatya	38.3367	38.2173	950	658
Manisa	38.6153	27.4049	71	726
Mardin	37.3103	40.7284	1040	996
Mersin	36.7808	34.6031	7	878
Muğla	37.2095	28.3668	646	428
Muş	38.7509	41.5023	1322	346
Nevşehir	38.6163	34.7025	1260	137
Niğde	37.9587	34.6795	1211	150
Ordu	40.9838	37.8858	5	187
Osmaniye	37.1021	36.2539	94	700
Rize	41.0400	40.5013	3	222
Sakarya	40.7676	30.3934	30	244
Samsun	41.3442	36.2564	4	210
Siirt	37.9319	41.9354	895	1062
Sinop	42.0299	35.1545	32	284
Sivas	39.7437	37.0020	1294	82
Şanlıurfa	37.1608	38.7863	550	1210
Şırnak	37.5209	42.4523	1350	908
Tekirdağ	40.9585	27.4965	4	242
Tokat	40.3312	36.5577	611	173
Trabzon	40.9985	39.7649	25	222
Tunceli	39.1058	39.5408	981	473
Uşak	38.6712	29.4040	919	173
Van	38.4693	43.3460	1675	135
Yalova	40.6589	29.2796	4	193
Yozgat	39.8243	34.8159	1301	44
Zonguldak	41.4492	31.7779	135	133

Results and discussion

In this study, the SARIMA model was used to perform monthly CDD forecasting data. CDD data for 81 provinces of Turkey, calculated monthly using meteorological data covering the period 1991–2022 and available on the website in [52], were used. Table 2 gives the geographical data for the 81 measurement stations or cities considered in this study. Figure 2 presents the locations of the 81 measurement stations on a map of Türkiye. Figure 3 presents the annual average air temperature map (1927–2021) of Türkiye. As seen in the figure, while the yearly average air temperatures in the cities of Ardahan, Erzurum, Kars, and Ağrı

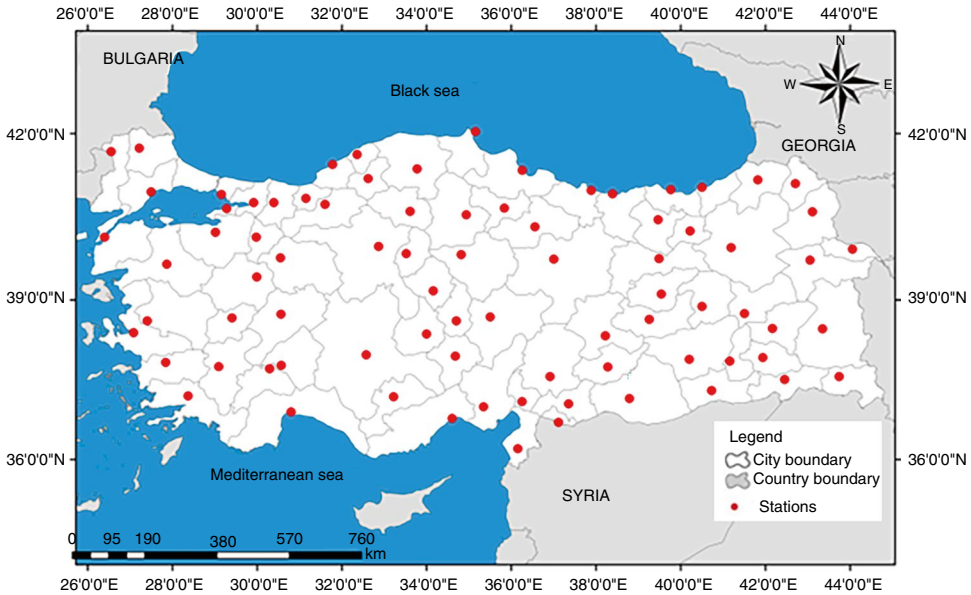


Fig. 2 Locations of the measurement stations on a map of Türkiye

in the Eastern Anatolian Region of Türkiye are quite low, the annual average temperatures in the cities of Şanlıurfa, Mersin, Adana, Antalya, Osmaniye, and in the Southeastern Anatolia and Mediterranean Regions are quite high. As seen in Fig. 4, the elevation values in Türkiye vary from region to region, and the elevation and rough terrain increase toward the east of the country. The mean elevation of the country is 1141 m, and the region where the elevation is maximum is the Eastern Anatolia Region. As a result, a wide variety of weather appear in Türkiye, as the annual average temperatures vary according to regions and altitudes. This means that CDD values will vary by region in Türkiye.

Figure 5a plots the monthly CDD values between January 1991 and December 2022 for Türkiye. CDD data show strong seasonality or periodicity throughout the year, as presented in the figure, but a linear upward trend is observed. Figure 5b presents the Box plot diagram of the CDD data according to the months of the year. It is clear from the figure that there is periodicity or seasonality over the year in the CDD data. Figure 5c, d shows the sample autocorrelation function (ACF) and partial autocorrelation function (PACF) plots of the CDD time series data. The autocorrelation results showed that lag 12 can be utilized in the forecasting model of the CDD values. This means that the seasonality period of the CDD data should be selected as $s = 12$. Consequently, to demonstrate the necessity of the SARIMA model, first-order seasonal differencing with period $s = 12$ and $D = 1$ was performed to convert the original data into the stationary condition.

Table 3 gives the Augmented Dickey–Fuller (ADF) test results of the original and transformed CDD data. The test results show that both ADF tests for the original data and transformed data achieve to decline null hypothesis that the CDD time series is trend stationary. To make CDD time series data more stationary, they were transformed into non-seasonal, normally, and seasonally differenced series. Following the first-order difference and seasonality procedures, the transformed CDD data analysis is displayed in Fig. 6.

The Akaike Information Criterion (AIC) was utilized to compare training models, and the Bayesian information criterion (BIC) was applied to identify the model with the best parsimonious sample fit. The minimum BIC and AIC values were selected as the decisive criteria to determine the most appropriate model using the Econometric Modeler application. Table 4 gives the most suitable SARIMA model and the resulting BIC and AIC values. As a result of different training applications, the SARIMA$(1,0,1)$x$(1,1,1)_{12}$ model was determined to be the best model satisfying the given conditions in the CDD time series forecasting model for Türkiye. Table 5 gives the output parameter results of the SARIMA$(1,0,1)$x$(1,1,1)_{12}$ model. Results show that AR,

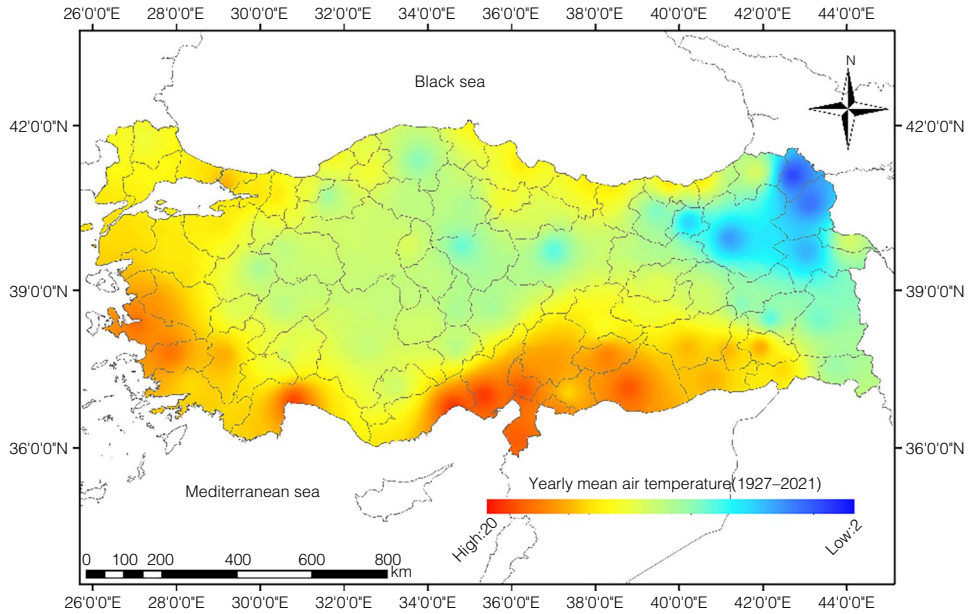


Fig. 3 Yearly average air temperature/°C map (1927–2021) of Türkiye

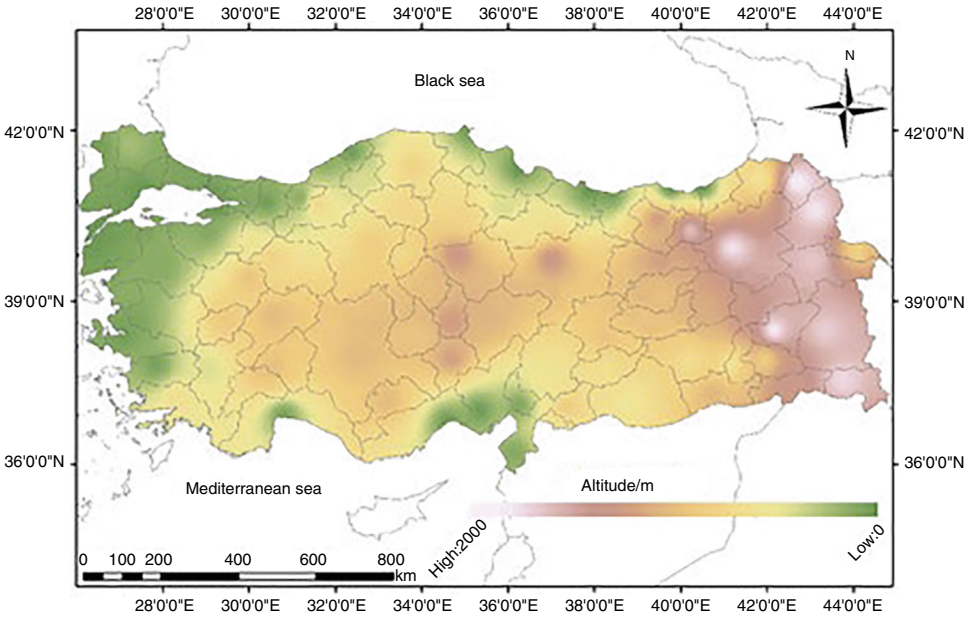


Fig. 4 Türkiye elevation map

MA, SAR, and MAR coefficients are significant at the 0.05 significance level.

Using the SARIMA $(1,0,1)x(1,1,1)_{12}$ model, the estimation values of the monthly average CDD data for Türkiye were determined from 1991 to 2040. The estimation outputs were compared with the actual data to assess the forecast performance of the SARIMA model. Figure 7 presents the historical and future trends of the monthly average CDD for Türkiye. As seen, the CDD values estimated by the SARIMA model are generally agree well with the actual data. Furthermore, it can be seen from the figure that there is a general increase in the monthly CDD values. Yearly average CDD values for the period 1991–2040 were calculated depending on the monthly CDD values for Türkiye. Figure 8 shows the yearly average CDD historical and future trends for Türkiye. As already observed in Fig. 7, a general increase in the yearly average CDD values has also been determined.

Figure 9 shows the variation in the monthly CDD against the respective monthly average air temperatures. CDD values can be directly correlated with the monthly average air

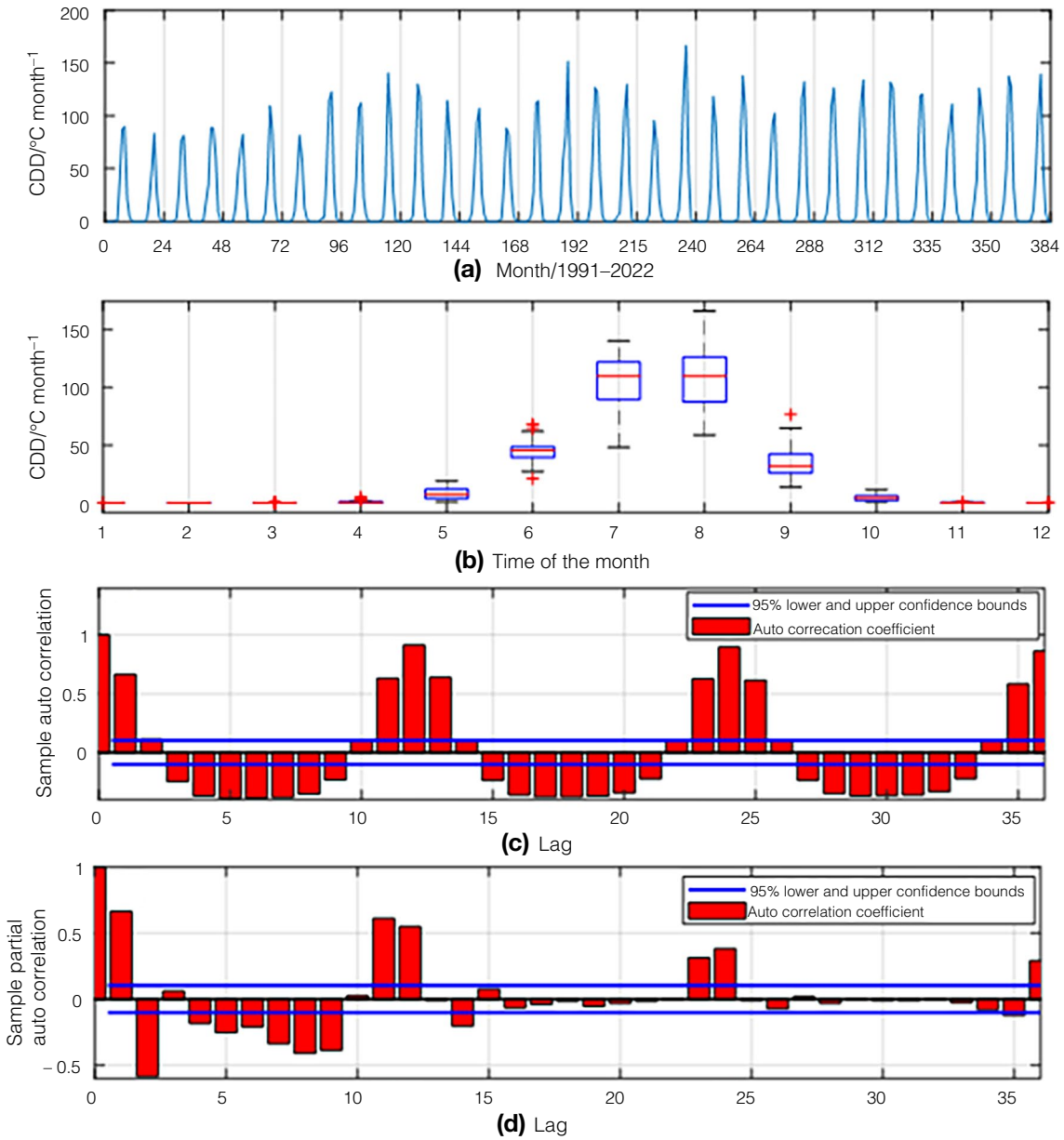


Fig. 5 Original data analysis for SARIMA model **a** Monthly average CDD historical trend in Türkiye (22 °C base temperature), **b** box plot of the times series data, **c** autocorrelation function graph of the times series data, **d** sample autocorrelation function graph of the times series data

Table 3 Results of the ADF test

Data	Null rejected	*P* value	Test statistic	Critical value	Lags	Model	Test statistic	Significant value
Original data	True	0.001	− 11.6855	− 1.9415	1	AR	*t*1	0.0500
Transformed data	True	0.001	− 20.2906	− 1.9415	1	AR	*t*1	0.0500

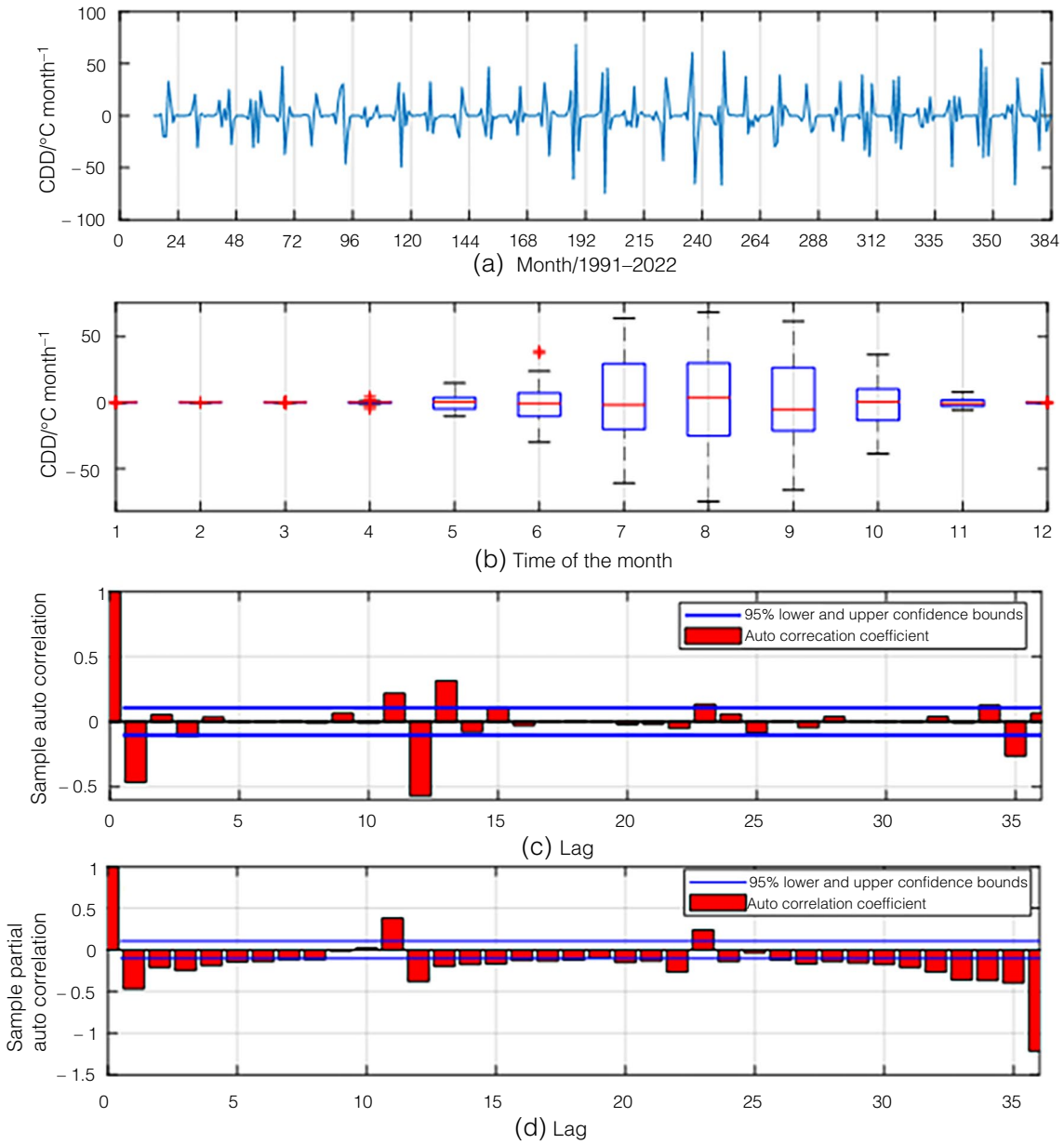


Fig. 6 Transformed data analysis after difference and seasonal processes **a** Monthly average CDD historical trend in Türkiye (22 °C base temperature), **b** box plot of the times series data, **c** autocorrelation function graph of the times series data, **d** sample autocorrelation function graph of the times series data

Table 4 Most suitable SARIMA model and the resulting BIC and AIC values

Model	BIC	AIC
SARIMA(1,0,1)x(1,1,1)$_{12}$	2874.4876	2855.0849

temperature, because of the large temperature difference with the selected base temperature of 22 °C. The correlation obtained in this figure can describe an average CDD for Türkiye without complex calculations.

Table 5 Output parameters for the SARIMA model

Parameter	Value	Standard error	*T* statistic	*P* value
Constant	0	0		
AR{1}	0.20332	0.037477	5.4253	5.7853e−08
SAR{12}	− 0.16512	0.029308	− 5.634	1.7611e−08
MA{1}	− 0.99471	0.0097478	− 102.0437	0
SMA{12}	− 0.77607	0.026341	− 29.463	8.5833e−191
Variance	96.6599	3.3413	28.9288	5.1928e−184

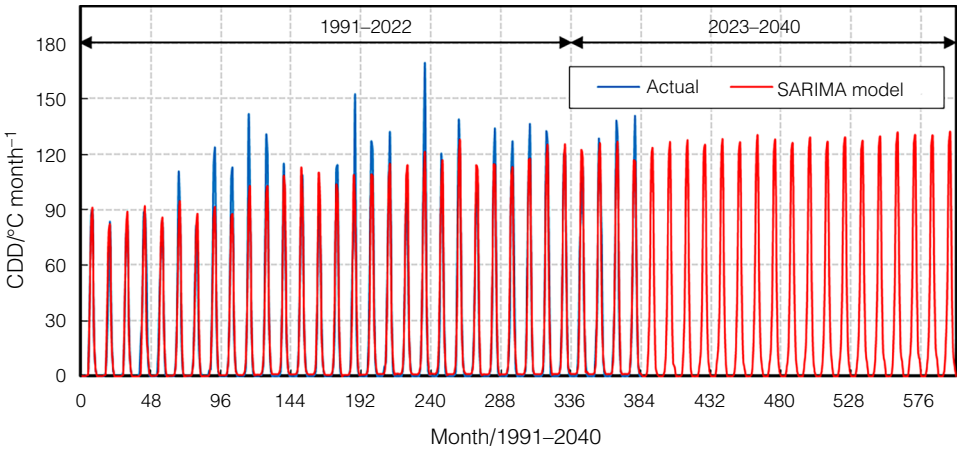


Fig. 7 Monthly average CDD historical and future trends for Türkiye

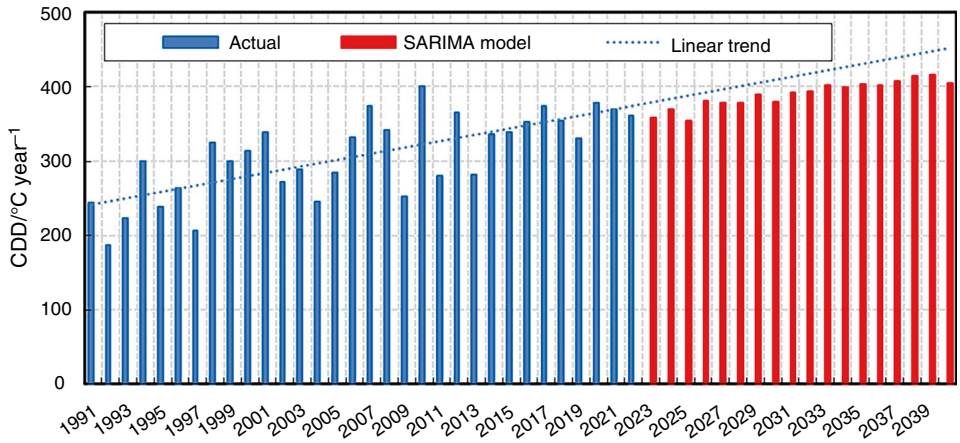


Fig. 8 Yearly average CDD historical and future trends for Türkiye

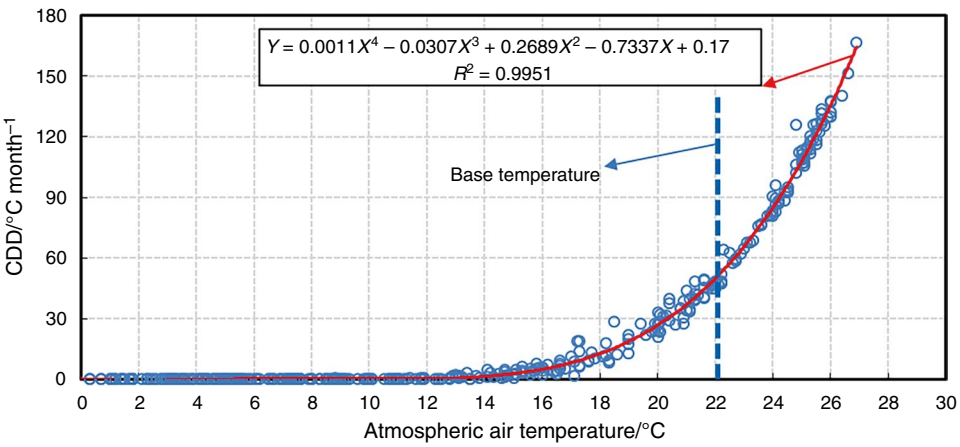


Fig. 9 Variation in the monthly CDD against the respective monthly average air temperature

Table 6 Results of the Engle's ARCH test

Model	Null rejected	*P* value	Test statistic	Critical value	Lags	Significance level
SARIMA(1,0,1)x(1,1,1)$_{12}$	true	0.004455	8.0882	3.8415	1	0.05

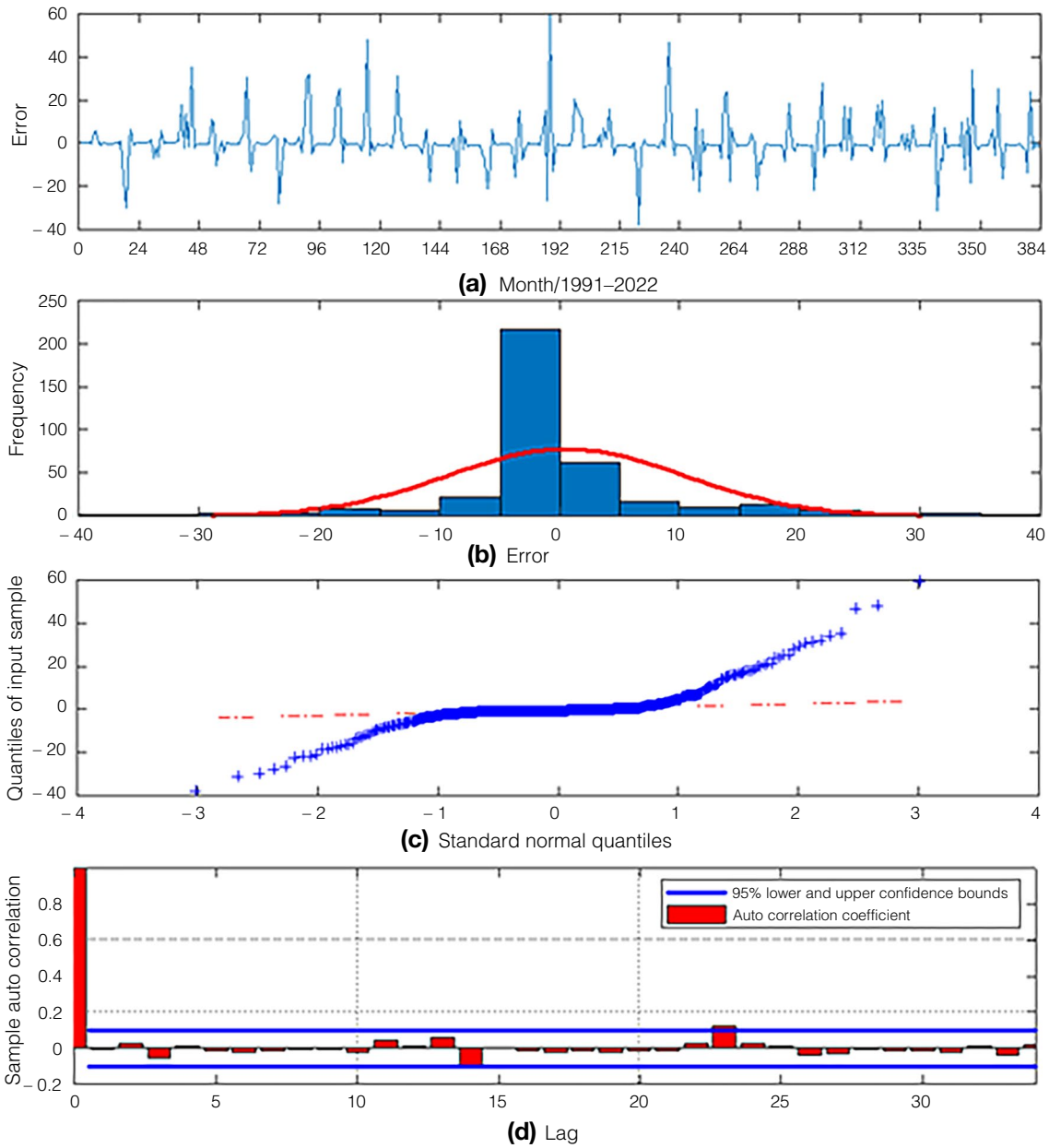


Fig. 10 Checking goodness of fit for residuals **a** time series plot, **b** normally distributed plot with constant mean and variance, **c** quantile–quantile plot, **d** uncorrelated sample ACF plot

To determine whether the SARIMA model adequately represents the statistical properties of the real CDD time series, a diagnostic check for the residuals of the SARIMA model was performed. In this regard, Engle's autoregressive conditional heteroskedasticity (ARCH) test was applied to the residuals of the SARIMA model. Table 6 gives Engle's ARCH test results for the residuals of the SARIMA model. The results suggest the rejection of the null hypothesis and

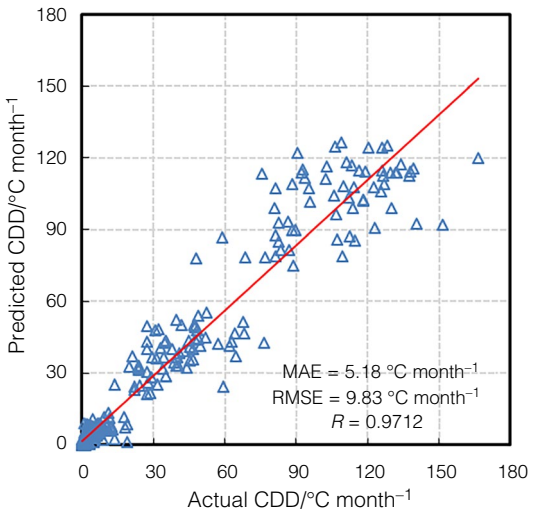


Fig. 11 Scatter plot of the monthly CDD values predicted by the SARIMA model with the actual data set

highlight that the residuals show no ARCH effects at the 5% significance level.

To ensure the reliability of the obtained SARIMA model, apart from Engle's ARCH test, time series, normality, autocorrelation, and heteroscedasticity of residual values were checked graphically. As seen in Fig. 10a, the residual time series plot reveals that the residuals have a mean of approximately zero with heteroscedastic properties. It is clear from Fig. 10b that the residuals are approximately reasonably normally distributed with constant mean and variance. The *Q*–*Q* plot in Fig. 10c shows that the residuals are approximately normal with slightly heavier tails. All sample autocorrelation values are roughly within the 95% lower and higher confidence ranges, as shown in Fig. 10d. The acquired results demonstrated that the residuals were homoscedastic, normally distributed, and serially uncorrelated and that they were roughly centered on zero. Figure 11 presents a scatter plot of the monthly CDD data estimated by the SARIMA model with the actual dataset. Results show that the predicted CDD values commonly agree with the actual CDD data. The MAE, RMSE, and R values of the model were obtained as 5.18 °C month^{-1}, 9.83 °C month^{-1}, and 0.9712, respectively. This means that the obtained SARIMA model is also suitable for future forecasting of the CDD in Türkiye.

Yearly CDD values were determined for the 81 city centers listed in Table 2. According to data based on 81 city centers maps of Türkiye's yearly CDD for 1991, 2006, and 2022 were drawn, as shown in Fig. 12. Then, a yearly CDD map was created on the basis of the average of the data between 1991 and 2022 (Fig. 13). As seen from the figures, the yearly CDD values vary significantly according to the region. Since the warmest provinces, in general, are found in the Southeastern Anatolia and Eastern Mediterranean regions of Türkiye, it is possible to note that the annual CDD values are highest in these regions. As expected, it is clear from the figures that the minimum cooling requirement is generally in the Central Anatolia, Eastern Anatolia, and Black Sea Regions of the country. The highest CDD values for the years 1991, 2006, and 2022 were obtained as 1023 °C year^{-1}, 1178 °C year^{-1}, and 1210 °C year^{-1}, respectively, in Şanlıurfa city located in the Southeastern Anatolia Region. On the other hand, the lowest CDD values for the same years were found as 0 °C year^{-1}, 3 °C year^{-1}, and 1 °C year^{-1}, respectively, in Ardahan city in the Eastern Anatolia Region. It is clearly seen on the maps in Fig. 12 that there is a general upward trend in yearly average CDD values over the years. The primary goal of this research is to simulate actual CDD data for Türkiye and estimate future values using the constructed model. Türkiye CDD time series data for the next years were revealed for this purpose utilizing the created SARIMA model. Future projections for the 216-month period (1 January 2023–31 December 2040) are shown in Fig. 7. In addition, Turkey's annual average CDD data are calculated until 2040 and are shown in Fig. 8. Maps of Türkiye's yearly CDD for the years 2030 and 2040 are presented in Fig. 14. The results show that CDD values for Türkiye will tend to increase in the coming years. For example, the annual average CDD value of Türkiye, which was 362.11 °C year^{-1} in 2022, is expected to exceed 400 °C year^{-1} in 2033 and reach a maximum level of 415.76 °C year^{-1} in 2039.

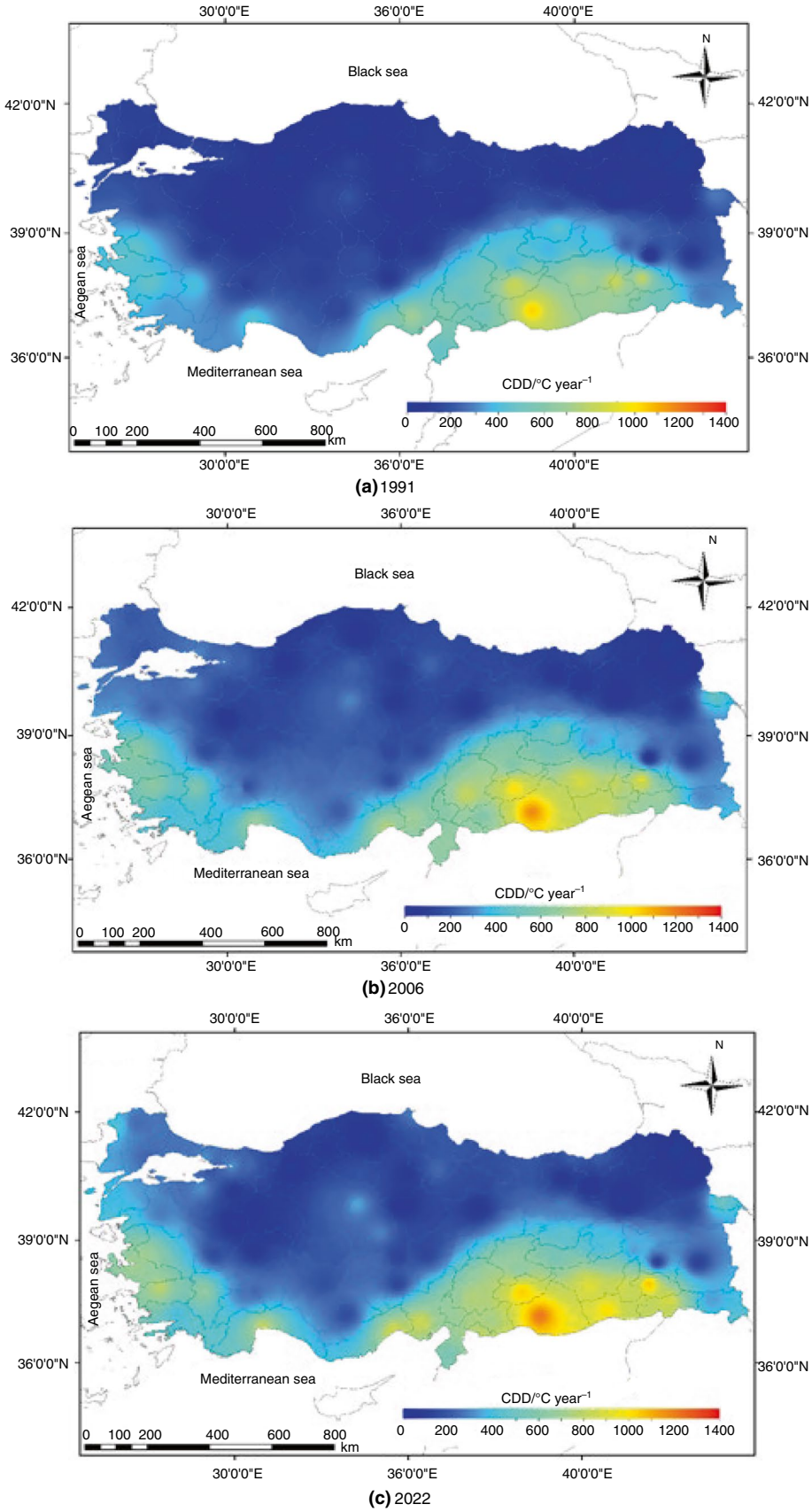


Fig. 12 Map of yearly CDD for Turkey with a 22 °C base temperature **a** 1991, **b** 2006, **c** 2022

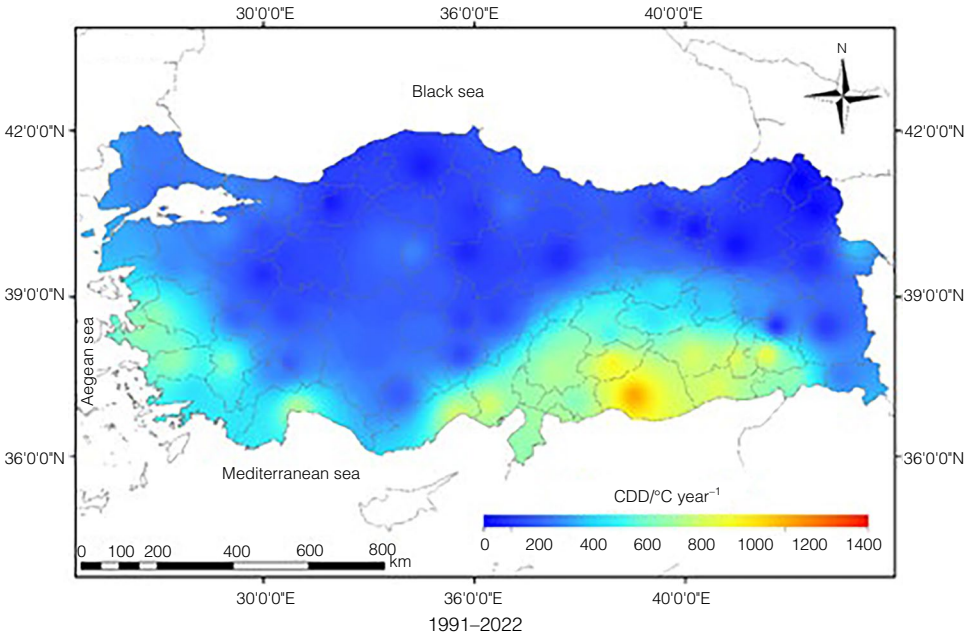


Fig. 13 Map of yearly CDD for Turkey based on the average of the data between 1991 and 2022 with a 22 °C base temperature

Designers create designs with user comfort in mind. Thermal comfort is one of these comforts that allow the user to use the building comfortably. As a shell that protects the building from various factors, the facade is critical in providing thermal comfort. The cooling loads of the building can be fulfilled by a facade designed in accordance with the physical environmental conditions. Temperature increases due to climate change, as demonstrated in the study, are a factor that the designer should consider during the initial design phase. The developed facade designs fulfill the necessary cooling load based on these temperature increases, thus contributing to energy savings.

The facade of a building, which generally refers to the front or exterior of a building, is essential in architecture and engineering because of its influence on energy efficiency. Furthermore, because of its impact on energy efficiency, the facade of a building is critical. The facade frequently is the most essential design feature in architecture because it dictates the structure of the remainder of the building. In this regard, CDD zones were created for buildings in Turkey in terms of facade design and energy efficiency based on the magnitude of the CDD values acquired in this study.

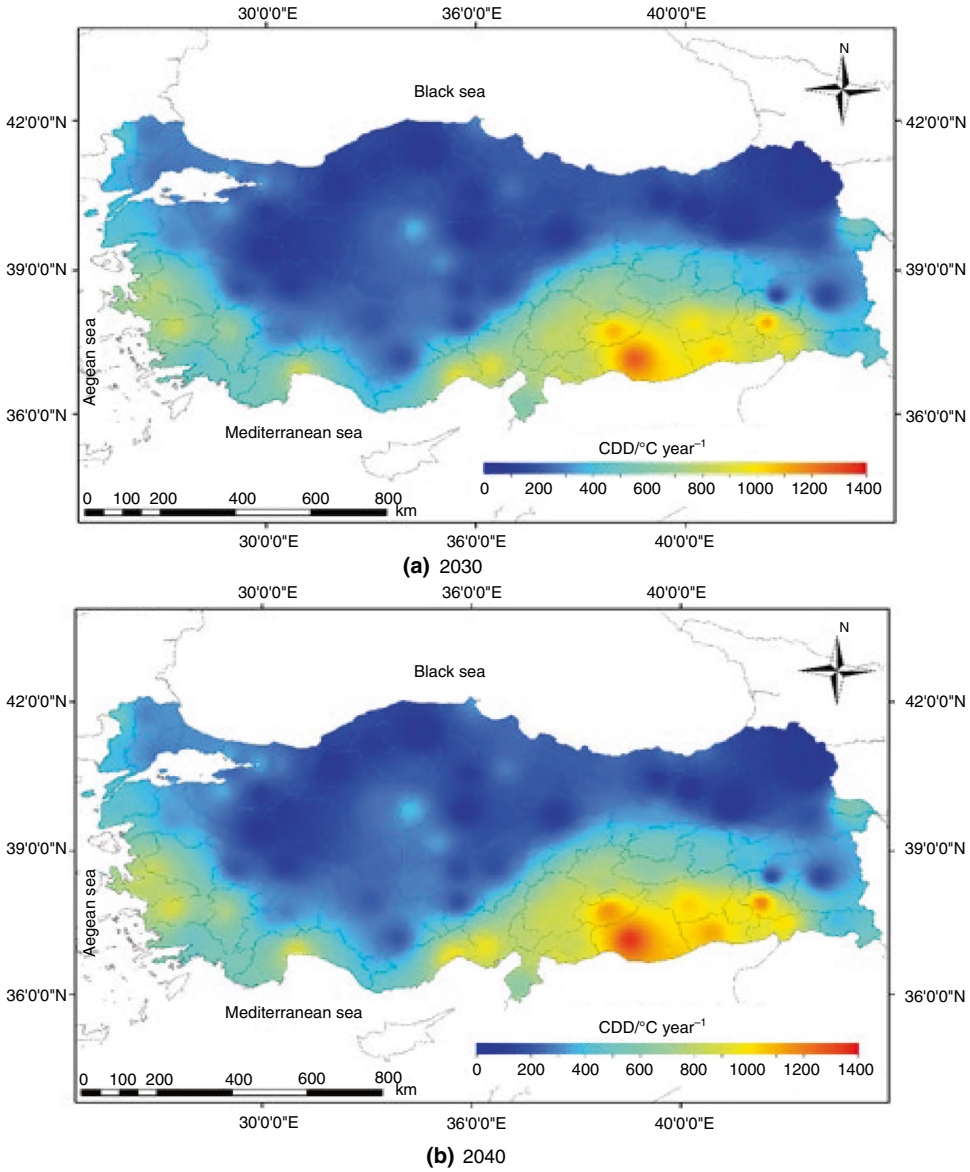


Fig. 14 Map of yearly CDD for Turkey with a 22 °C base temperature **a** 2030, **b** 2040

Zone I was designated as CDD ≤ 250 °C year^{-1}, Zone II as 251 °C year^{-1} ≤ CDD ≤ 500 °C year^{-1}, and Zone III as CDD ≥ 501 °C year^{-1}. Figure 15 depicts the CDD regions created for the years 2022 and 2040. Zone I is the zone with the least cooling required. Zone II denotes areas that require greater cooling than Zone I. Zone III, on the other hand, depicts areas where cooling is crucial. In 2022, Zone III includes the cities of Adana, Adıyaman, Antakya, Antalya, Aydın, Batman, Denizli, Diyarbakır, Gaziantep, Iğdır, İzmir, Kahramanmaraş, Kilis, Malatya, Manisa, Mardin, Mersin, Osmaniye, Siirt, Şanlıurfa, and Şırnak. Zone III's borders are expected to enlarge in 2040, adding the province of Tunceli to its boundaries. It is necessary to place a greater emphasis on the most appropriate facade design in terms of energy efficiency for the cooling needs of the buildings to be built for the provinces that include this region, which has grown in size since today.

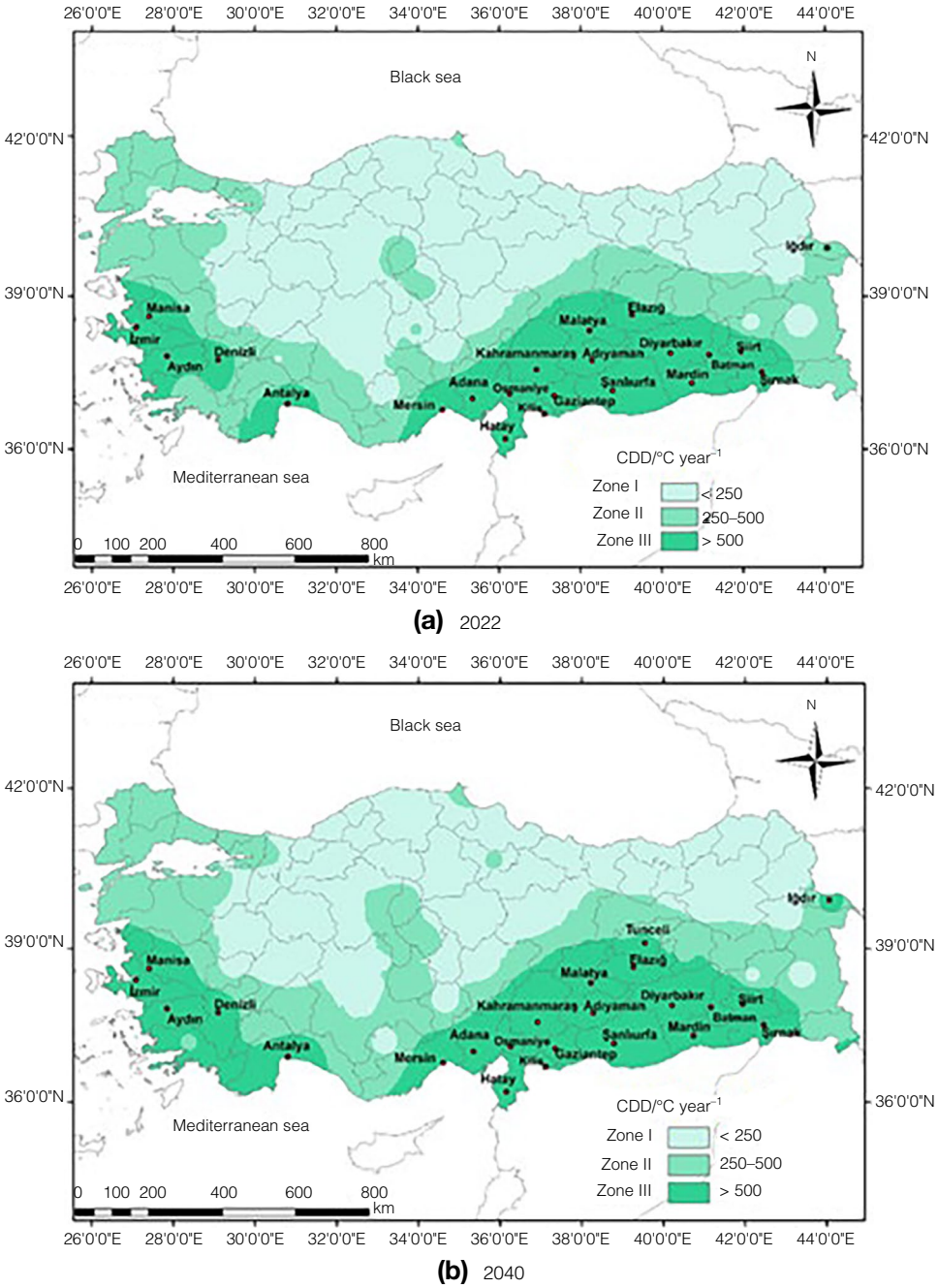


Fig. 15 CDD zones for the buildings in Turkey in terms of facade design and energy efficiency

Conclusions

It is imperative that countries create simplified forecasting models, considering future climatic conditions, to take appropriate policy measures and develop energy consumption scenarios that guarantee the highest energy savings. In this regard, analysis of the historical evolution of CDD values in any region is critical for determining the current state and future trends of energy consumption in that region. The facade of a building can be defined as faces that establish the connection between the interior and exterior of buildings and provide control against the physical environment. In this context, facades play an important role in issues such as esthetics, structural, and protection from external influences. In this study, historical trends, current state, and future forecasts of CDD in Türkiye were performed to develop an optimum facade design for buildings. CDD values were calculated using daily average temperature data measured at meteorological stations in 81 city centers of Türkiye for the period 1991–2022. The base temperature was considered as 22 °C in the calculations. CDD data were modeled using the SARIMA approach, and a time series forecasting

model was performed for Türkiye. With this time series SARIMA model, future trends in CDD were predicted for the period 2023–2040. In the developed time series model of Türkiye's CDD data, in general, the basic time series features that characterize the long-term increase/decrease trend, periodic seasonal behavior, and stochastic behavior of the data were considered. With the help of the ArcGIS software program, yearly CDD maps of Türkiye were created for 1991, 2006, 2022, 2030, and 2040, and the historical and regional changes in CDD values throughout Turkey were visually revealed. The obtained results reveal that due to global warming, yearly CDD values in Türkiye generally show an increasing trend in the period 1991–2022, and this increasing trend is expected to continue in the 2023–2040 period. Architects and engineers can fulfill their net zero-emission building targets by designing with this information in mind.

It is widely known that heating, cooling, and lighting systems within buildings account for a significant portion of total energy consumption. The building facade is among the crucial components aimed at minimizing this energy usage. The strategic incorporation of transparent areas and shadow elements into the facade allows for controlled daylight utilization, thereby reducing the demand for artificial lighting. Furthermore, effective management of solar energy gain plays a pivotal role in achieving optimal thermal comfort and minimizing heating and cooling requirements. Contemporary advancements in facade design involve rigorous research, employing specialized software, simulation programs, and genetic algorithms to optimize various facade parameters. Given Turkey's predominantly sunny climate, designing buildings with daylight considerations is particularly pertinent. In future studies, it is aimed to use daylight and solar radiation at an optimum level in buildings in Turkey by focusing on visual and thermal comfort. Using meteorological data analysis and appropriate software, scenarios will be developed to determine the optimal facade configurations for maximizing daylight utilization.

Author contributions All authors contributed to the study conception and design. Material preparation, data collection, and analysis were performed by AB, KÇ, and MB. The first draft of the manuscript was written by AB, and all authors commented on previous versions of the manuscript. All authors read and approved the final manuscript.

Funding Open access funding provided by the Scientific and Technological Research Council of Türkiye (TÜBİTAK). The authors declare that no funds, grants, or other support was received during the preparation of this manuscript.

Data availability The data and materials that support the findings of this study are available from the corresponding author.

Declarations

Conflict of interest The authors have no relevant financial or non-financial interests to disclose.

Ethical approval All authors confirm that the submitted work is original and has not been published elsewhere in any form or language (in part or in whole).

Open Access This article is licensed under a Creative Commons Attribution 4.0 International License, which permits use, sharing, adaptation, distribution and reproduction in any medium or format, as long as you give appropriate credit to the original author(s) and the source, provide a link to the Creative Commons licence, and indicate if changes were made. The images or other third party material in this article are included in the article's Creative Commons licence, unless indicated otherwise in a credit line to the material. If material is not included in the article's Creative Commons licence and your intended use is not permitted by statutory regulation or exceeds the permitted use, you will need to obtain permission directly from the copyright holder. To view a copy of this licence, visit http://creativecommons.org/licenses/by/4.0/.

References

1. DeAngelo J, Azevedo I, Bistline J, et al. Energy systems in scenarios at net-zero CO_2 emissions. Nat Commun. 2021;12:6096.
2. REN21 (2022) Global status report. https://www.ren21.net/reports/global-status-report/. (Accessed 25 December 2022)
3. Işık E, İnallı M, Celik E. ANN and ANFIS approaches to calculate the heating and cooling degree day values: the case of provinces in Turkey. Arab J Sci Eng. 2019;44(9):7581–97.
4. Papakostas KT, Pavlou S, Papadopoulos AM. Ambient air temperature and degree-day data analysis of the period 2006–2017 for Cyprus. J Therm Anal Calorim. 2020;141:435–45.
5. Satman A, Yalcinkaya N. Heating and cooling degree-hours for Turkey. Energy. 1999;24(10):833–40.
6. Kuru M, Calis G. Application of time series models for heating degree day forecasting. Organ Technol Manag Constr Int J. 2020;12(1):2137–46.
7. Dombaycı ÖA. Degree-days maps of Turkey for various base temperatures. Energy. 2009;34(11):1807–12.
8. Regis M, Serra P, van den Heuvel ER. Random autoregressive models: a structured overview. Econom Rev. 2022;41(2):207–30.
9. Kuranga C, Pillay N. A comparative study of nonlinear regression and autoregressive techniques in hybrid with particle swarm optimization for time-series forecasting. Expert Syst Appl. 2022;190: 116163.
10. Shadab A, Said S, Ahmad S. Box–Jenkins multiplicative ARIMA modeling for prediction of solar radiation: a case study. Int J Energy Water Resour. 2019;3(4):305–18.
11. Khatibi R, Ghorbani MA, Naghipour L, Jothiprakash V, Fathima TA, Fazelifard MH. Inter-comparison of time series models of lake levels predicted by several modeling strategies. J Hydrol. 2014;511:530–45.
12. Ghorbani MA, Deo RC, Karimi V, et al. Design and implementation of a hybrid MLP-GSA model with multi-layer perceptron-gravitational search algorithm for monthly lake water level forecasting. Stoch Environ Res Risk Assess. 2019;33:125–47.
13. Jafarzadeh AA, Pal M, Servati M, FazeliFard MH, Ghorbani MA. Comparative analysis of support vector machine and artificial neural network models for soil cation exchange capacity prediction. Int J Environ Sci Technol. 2016;13(1):87–96.

14. Ghorbani MA, Khatibi R, Goel A, FazeliFard MH, Azani A. Modeling river discharge time series using support vector machine and artificial neural networks. Environ Earth Sci. 2016;75(8):1–13.
15. Yildirim A, Bilgili M, Ozbek A. One-hour-ahead solar radiation forecasting by MLP, LSTM, and ANFIS approaches. Meteorol Atmos Phys. 2023;135:10.
16. Bilgili M, Ilhan A, Ünal Ş. Time-series prediction of hourly atmospheric pressure using ANFIS and LSTM approaches. Neural Comput Appl. 2022;34:15633–48.
17. Ghorbani MA, Deo RC, Yaseen ZM, et al. Pan evaporation prediction using a hybrid multilayer perceptron-firefly algorithm (MLP-FFA) model: case study in North Iran. Theor Appl Climatol. 2018;133:1119–31.
18. Kavousi-Fard A, Samet H, Marzbani F. A new hybrid modified firefly algorithm and support vector regression model for accurate short term load forecasting. Expert Syst Appl. 2014;41(13):6047–56.
19. De Rosa M, Bianco V, Scarpa F, Tagliafico LA. Historical trends and current state of heating and cooling degree days in Italy. Energy Convers Manag. 2015;90:323–35.
20. Sadeqi A, Tabari H, Dinpashoh Y. Spatio-temporal analysis of heating and cooling degree days over Iran. Stoch Environ Res Risk Assess. 2022;36:869–91.
21. Yildiz I, Sosaoglu B. Spatial distributions of heating, cooling, and industrial degree-days in Turkey. Theor Appl Climatol. 2007;90:249–61.
22. Al-Hadhrami LM. Comprehensive review of cooling and heating degree days characteristics over Kingdom of Saudi Arabia. Renew Sustain Energy Rev. 2013;27:305–14.
23. Papakostas K, Kyriakis N. Heating and cooling degree-hours for Athens and Thessaloniki, Greece. Renew Energy. 2005;30:1873–80.
24. Idchabani R, Garoum M, Khaldoun A. Analysis and mapping of the heating and cooling degree-days for Morocco at variable base temperatures. Int J Ambient Energy. 2015;36(4):190–8.
25. Jiang F, Li X, Wei B, Hu R, Li Z. Observed trends of heating and cooling degree-days in Xinjiang Province, China. Theor Appl Climatol. 2009;97:349–60.
26. Büyükalaca O, Bulut H, Yılmaz T. Analysis of variable-base heating and cooling degreedays for Turkey. Appl Energy. 2001;69:269–83.
27. Livada I, Pyrgou A, Haddad S, Sadeghi M, Santamouris M. Recent climatic trends and analysis of monthly heating and cooling degree hours in Sydney. Climate. 2021;9(7):114.
28. Li Y, Li J, Xu A, Feng Z, Hu C, Zhao G. Spatial–temporal changes and associated determinants of global heating degree days. Int J Environ Res Public Health. 2021;18(12):6186.
29. Indraganti M, Boussaa D. A method to estimate the heating and cooling degree-days for different climatic zones of Saudi Arabia. Build Serv Eng Res Technol. 2017;38(3):327–50.
30. Amber KP, Aslam MW, Ikram F, Kousar A, Ali HM, Akram N, et al. Heating and cooling degree-days maps of Pakistan. Energies. 2018;11(1):94.
31. Ramon D, Allacker K, De Troyer F, Wouters H, van Lipzig NP. Future heating and cooling degree days for Belgium under a high-end climate change scenario. Energy Build. 2020;216: 109935.
32. OrtizBeviá MJ, Sánchez-López G, Alvarez-Garcìa FJ, Ruiz-deElvira A. Evolution of heating and cooling degree-days in Spain: trends and interannual variability. Glob Planet Change. 2012;92:236–47.
33. Andrade C, Mourato S, Ramos J. Heating and cooling degree-days climate change projections for Portugal. Atmosphere. 2021;12(6):715.
34. Ukey R, Rai AC. Impact of global warming on heating and cooling degree days in major Indian cities. Energy Build. 2021;244: 111050.
35. Corrales-Suastegui A, Ruiz-Alvarez O, Torres-Alavez JA, Pavia EG. Analysis of cooling and heating degree days over Mexico in present and future climate. Atmosphere. 2021;12(9):1131.
36. Spinoni J, Vogt JV, Barbosa P, Dosio A, McCormick N, Bigano A, Füssel HM. Changes of heating and cooling degree-days in Europe from 1981 to 2100. Int J Climatol. 2018;38:e191–208.
37. Cao J, Shi J, Li M, Zhai Z, Zhang R, Wang M. Variations of cooling and dehumidification degree days in major climate zones of china during the past 57 years. Atmosphere. 2023;14(4):752.
38. Omarov B, Memon SA, Kim J. A novel approach to develop climate classification based on degree days and building energy performance. Energy. 2023;267: 126514.
39. Pangsy-Kania S, Biegańska J, Flouros F, Sokół A. Heating and cooling degree-days vs climate change in years 1979–2021. Evidence from the European Union and Norway. Ekonomia i Środowisko. 2024;88(1):1–25.
40. Islam ARMT, Ahmed I, Rahman MS. Trends in cooling and heating degree-days overtimes in Bangladesh? An investigation of the possible causes of changes. Nat Hazards. 2020;101(3):879–909.
41. Al-Saadi S, Al-Rawas G, Gunawardhana L, Al-Farsi N, Al-Kalbani H. Developing climate classification for Oman using degree-days method. Arab J Sci Eng. 2023;48(9):11391–405.
42. Salem H, Khanafer K, Alshammari M, Sedaghat A, Mahdi S. Cooling degree days for quick energy consumption estimation in the GCC countries. Sustainability. 2022;14(21):13885.
43. Bilgili M, Canpolat C, Pinar E, et al. Analysis of heating degree-days (HDD) data using machine learning and conventional time series methods. Theor Appl Climatol. 2023. https://doi.org/10.1007/s00704-023-04543-9.
44. Bilgili M. Time series forecasting on cooling degree-days (CDD) using SARIMA model. Nat Hazards. 2023. https://doi.org/10.1007/s11069-023-06109-4.
45. Karagiannidis A, Lagouvardos K, Kotroni V, Galanaki E. Expected changes in heating and cooling degree days over Greece in the near future based on climate scenarios projections. Atmosphere. 2024;15(4):393.
46. Karagiannids A, Lagouvardos K, Kotroni V, Galanaki E. Analysis of current and future heating and cooling degree days over Greece using observations and regional climate model simulations. Environ Sci Proc. 2023;26(1):149.
47. Mehmood S, Amber KP, Usman M, Friedrich D. Integrating latent load into the cooling degree days concept for current and future weather projections. Buildings. 2023;14(1):106.
48. Miranda ND, Lizana J, Sparrow SN, Zachau-Walker M, Watson PA, Wallom DC, et al. Change in cooling degree days with global mean temperature rise increasing from 1.5 C to 2.0 C. Nat Sustain. 2023;6(11):1326–30.
49. Escandón R, Ferrari S, Blázquez T, Suárez R. Assessment of vulnerability to overheating at a regional scale through parametric simulation models and cooling degree-days analysis: the case of southern Spanish social housing stock. J Build Eng. 2023;73: 106709.
50. Box GE, Jenkins GM. Time series analysis: forecasting and control. 3rd ed. Englewood Cliffs: Prentice Hall; 1994.
51. Bilgili M, Keiyinci S, Ekinci F. One-day ahead forecasting of energy production from run-of-river hydroelectric power plants with a deep learning approach. Sci Iran. 2022;29(4):1838–52.
52. TSMS (2023) Turkish State Meteorological Service. https://www.mgm.gov.tr/

Publisher's Note Springer Nature remains neutral with regard to jurisdictional claims in published maps and institutional affiliations.